

Accepted Manuscript

On the formation and structural properties of hexagonal rare earth (Y, Gd, Dy, Er and Yb) disilicide thin films

F.A. Geenen, W. Knaepen, J. Demeulemeester, K. De Keyser, J.L. Jordan-Sweet, C. Lavoie, A. Vantomme, C. Detavernier

PII: S0925-8388(14)00972-4

DOI: <http://dx.doi.org/10.1016/j.jallcom.2014.04.142>

Reference: JALCOM 31107



To appear in:

Received Date: 5 December 2013

Revised Date: 19 April 2014

Accepted Date: 21 April 2014

Please cite this article as: F.A. Geenen, W. Knaepen, J. Demeulemeester, K. De Keyser, J.L. Jordan-Sweet, C. Lavoie, A. Vantomme, C. Detavernier, On the formation and structural properties of hexagonal rare earth (Y, Gd, Dy, Er and Yb) disilicide thin films, (2014), doi: <http://dx.doi.org/10.1016/j.jallcom.2014.04.142>

This is a PDF file of an unedited manuscript that has been accepted for publication. As a service to our customers we are providing this early version of the manuscript. The manuscript will undergo copyediting, typesetting, and review of the resulting proof before it is published in its final form. Please note that during the production process errors may be discovered which could affect the content, and all legal disclaimers that apply to the journal pertain.

Keywords: rare earth silicide, thin films, x-ray diffraction, solid state reaction, crystal structure

ACCEPTED MANUSCRIPT

On the formation and structural properties of hexagonal rare earth (Y, Gd, Dy, Er and Yb) disilicide thin films

F.A. Geenen^{a,*}, W. Knaepen^a, J. Demeulemeester^b, K.De Keyser^a, J.L. Jordan-Sweet^c, C. Lavoie^c, A. Vantomme^b, C. Detavernier^a

^a*Department of Solid-State Sciences, Ghent University, 9000 Gent, Belgium*

^b*Instituut voor Kern- en Stralingsfysica, KU Leuven, B-3001 Leuven, Belgium*

^c*IBM T.J. Watson Research Center, Yorktown Heights, NY, USA*

Abstract

A systematic study was performed of the solid state reaction between a 100 nm thick layer of a rare earth metal and a Si substrate. The solid state reaction of five different rare earth metals (yttrium, gadolinium, dysprosium, erbium and ytterbium) were studied by *in situ* X-ray diffraction measurements on Si(100), Si(111) and poly-Si. This allowed us to make a comparison between the different systems. The formation temperature of h-RESi_{1.7} are the highest on Si(111) and the lowest on poly-si for all examined RE metals. Additionally, the texture of the Gd disilicide phase on Si(100) and Si(111) was investigated by means of *ex situ* pole figure measurements. The epitaxial relationship of hexagonal GdSi_{1.7} and orthorhombic GdSi₂ on the different Si substrates is determined. The epitaxial growth is the strongest on Si(111).

1. Introduction

Rare earth silicides (RES) are often reported as a separate subgroup of the silicides as they display similar distinct and peculiar properties [1]. RES gained considerable attention in the early 80's after the Schottky barrier height (SBH) of RES contacts on Si was reported to be amongst the lowest (0.3 - 0.4 eV) and the highest (0.7 - 0.8 eV) of the reported SBH on n- and p-type Si respectively [2, 3]. The exceptionally SBH, in combination with a

*Corresponding author. Tel.: +32 9264 4370

Email address: Filip.Geenen@UGent.be (F.A. Geenen)

good electrical conductivity and the possibility to grow epitaxially on Si(111) [4], rendered these silicides interesting candidates for contacting applications in microelectronics. The integration of RES proved difficult, i.e. because of their high affinity for oxygen [5] and the formation of pinholes [6], something that can be countered by, amongst other solutions, the use of a capping layer.

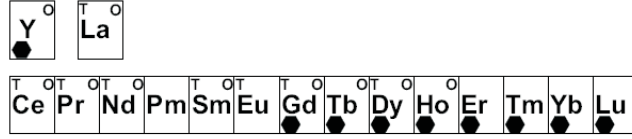


Figure 1: Overview of the different crystal structures of the rare earth disilicide phases. T stands for tetragonal $ThSi_2$ structure, the hexagon is the defective AlB_2 structure and O represents the orthorhombic $GdSi_2$ structure [7, 6]. Grayed elements are the elements which we examined in this paper.

$MSi_{1.7}$	a (Å)	c (Å)	η (%)
$GdSi_{1.7}$	3.877	4.172	+0.960
$YSi_{1.7}$	3.842	4.140	+0.052
$DySi_{1.7}$	3.831	4.121	-0.234
$ErSi_{1.7}$	3.798	4.088	-1.090
$YbSi_{1.7}$	3.784	4.098	-1.460

Table 1: Lattice parameters of the hexagonal RE silicides studied in this work, together with their room temperature lattice mismatch with the d-spacing between the Si(111) planes ($\eta = \frac{a_{Si} - a_{RE}}{a_{Si}}$, with $a_{Si} = 3.840$) [8].

The RE thin films are reported to crystallize in three different structures: tetragonal $ThSi_2$, orthorhombic $GdSi_2$ and hexagonal AlB_2 , as shown in Fig. 1 [2, 7]. The lightest RE metals only form a tetragonal or orthorhombic lattice, although the addition of a fraction of another RE species can force this ternary system into a hexagonal lattice structure [9]. The intermediate RE metals first form a defective hexagonal structure but transform into a tetragonal or orthorhombic structure at higher temperatures, whereas the RE metals heavier than Ho only form the hexagonal AlB_2 .

The focus in this article lies on RES with a AlB_2 structure as these are reported to grow epitaxially on the Si(111) substrate [4], which can be interesting for the use as an interlayer in microelectronic devices. This can

be related to the three-fold symmetry of Si {111}. The ordering of the Si atoms in this plane is then in good agreement with the lattice parameters of the hexagonal stacking of the AlB_2 structure, as listed in Table 1 for the relevant RES in this article. It should be stressed that the Si-sublattice in the hexagonal AlB_2 structure of RES is reported to be vacancy-rich (about 15% of ordered vacancies), so the alternative notation $\text{h-RESi}_{1.7}$ or h-RESi_{2-x} is more justifiable.

Another distinction between the RES and other metal silicides is the way that the first phase is formed during a thermal anneal. Whereas normally the first phase formation is limited by the diffusion of one of the components into the other, a solid state reaction between a thin RE metal film and a Si substrate has been reported to be nucleation controlled [10] for the rare earth metals. This is characterised by a threshold temperature, below which no silicidation is observed and above which the silicidation is completed almost instantaneously.

In this paper, the silicidation reaction of 5 different RE metals (Y, Gd, Dy, Er and Yb) is studied using *in situ* XRD. As the hexagonal $\text{RESi}_{1.7}$ phase is reported to grow epitaxially on Si(111), the first criterion in the selection of the RE metals was the reported formation of this hexagonal phase. Secondly, the RE metals were selected to cover a broad range of lattice parameters (Table 1) as one of the important parameters which influences textured growth is the lattice (mis)match between the growing film and the substrate. The silicides formed during a ramp anneal are studied on polycrystalline Si, Si(100) and Si(111) substrates by means of *in situ* XRD. The identification of the phases is much easier on poly-Si, since the substrate grains are randomly oriented and the XRD-measurements can detect most, if not all, diffraction peaks. The phases are identified on poly-Si, as in that case the influence of the substrate orientation on the film texture can be neglected. The effect of the different substrates is then discussed by comparing the *in situ* XRD measurements. For the case of Gd, the texture of the hexagonal and orthorhombic disilicide phase is investigated on Si(100), and Si(111) through *in situ* XRD and *ex situ* pole figures.

2. Experimental procedures

The p-type Si(100), Si(111) and polycrystalline Si (poly-Si) substrates were chemically cleaned following the RCA-procedure and subjected to a 20 s dip in 2% diluted HF prior to being loaded into the deposition sys-

tems. For Y, Gd, Dy and Er, a 100 nm metal film was deposited at a rate of about 0.2 \AA/s using Molecular Beam Epitaxy in an ultra high vacuum system ($6.6 \cdot 10^{-8} \text{ Pa}$). Due to the absence of Yb as a source material for molecular beam epitaxy, an Yb film with the same thickness was sputter-deposited at a deposition rate of 1.3 \AA/s in a $5 \times 10^{-1} \text{ Pa}$ Ar atmosphere after reaching a base pressure of 10^{-4} Pa in a sputter deposition system. To prevent oxidation of the deposited RE-metals, a 10 to 12 nm Si capping layer was deposited on all samples without breaking the vacuum. The influence of this amorphous capping layer on the phase formation is considered small, due to the relative small thickness of the capping layer in respect of the RE-metal layer. However, one should be careful when to compare the following results with rare earth thin film experiments that do not use a capping layer.

The silicidation process was studied using the *in situ* XRD setup at the X20C beam line of the National Synchrotron Light Source (NSLS) at Brookhaven National Laboratory. The samples were heated from room temperature to $950 \text{ }^\circ\text{C}$ in a purified He ambient using a $3 \text{ }^\circ\text{C/s}$ ramp anneal. The temperatures were recorded by means of a thermocouple placed in a molybdenum layer just beneath the sample. Since the position of the incident X-ray beam is fixed relative to the heater, the measurements are reproducible and systematic errors are cleared out after calibrating the temperature measurements with the temperature anneal of several eutectic materials on a HF-cleaned Si substrate (Al, Au, Ag on HF-cleaned Si substrates). The energy of the X-rays was selected at 6.9 keV ($\lambda = 0.180 \text{ nm}$) with an energy resolution of 1.5% using a multilayer monochromator and a spot-size of 1 by 2 mm. XRD patterns were obtained every 0.5 s using a linear detector covering about 14° in 2θ . Because of the fixed position of the incident X-rays, sample and detector (Bragg-Brentano geometry), the *in situ* XRD measurements only detects X-rays diffracted from crystalline planes nearly parallel to the surface. If a grain lacks such planes parallel to the surface, it will not contribute to the measured XRD. Consequently, the *in situ* XRD measurements will miss highly textured phases.

To study the (possibly) textured formation of RE silicides, the preferred orientation of grains in Gd/Si samples was studied as a function of silicon substrate orientation (e.g. Si(100) and Si(111)) using XRD pole figure measurements at the X20-A beamline. Pole figures are obtained by measuring the diffracted intensity at a given diffraction angle 2θ between the beam source and the x-ray detector, while tilting and rotating the sample over a range of angles χ and Φ , respectively, using an Euler cradle [11]. The value of 2θ can

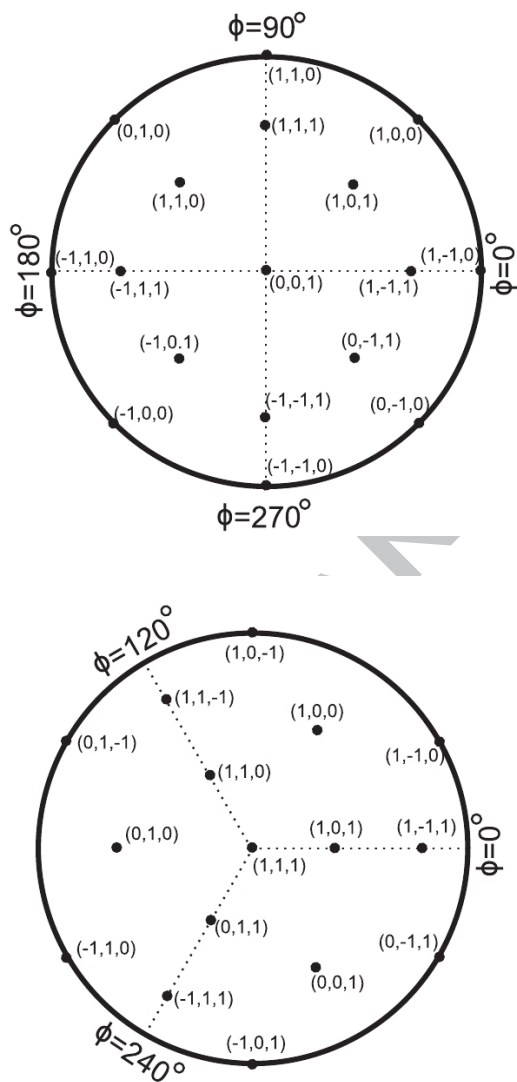


Figure 2: The location of low-index poles of Si(100) (top) and Si(111) (bottom).

be related to a specific $\{hkl\}$ lattice plane of a certain phase, and by plotting the data as a function of angles χ and Φ for a single value of 2θ , a statistical distribution as a function of preferred orientation is deduced for the corresponding $\{hkl\}$ plane. Strongly textured phases that are not detectable in the *in situ* XRD measurement, can be detected by the analysis of pole figures. In this work, pole figures were measured using an x-ray wavelength of $\lambda = 0.154$ nm, as selected using a Ge(111) double-crystal monochromator. The diffracted x-rays were detected using a custom linear detector (8 cm Si strip detector, 640 pixels) which allows the simultaneous acquisition of pole figures covering 2θ values in a 42° range. The pole figures were acquired in steps of 0.5° in χ and Φ ($0 \leq \chi \leq 85^\circ$ and $0 \leq \Phi \leq 90^\circ$ for Si(100) or $0 \leq \Phi \leq 120^\circ$ for Si(111)). The complete pole figures were obtained by tiling the measured data to the full range $0 \leq \Phi \leq 360^\circ$, as the pole figures share the same rotational symmetry of the substrate. The samples were positioned such that the Si poles are at the Φ and χ locations as shown in Fig. 2. The features on the pole figures can then be used to identify the various types of texture that are present in the film. The preferential orientations were fitted with GUSTAV[12], a software package for thin film texture analysis.

3. Results

3.1. The solid state reaction between Gd and Si

In this section, we report the results of the phase formation of Gd on silicon and the effect of different substrate orientations. This will be done mainly by means of *in situ* XRD-measurements and pole figures. After this section, an expansion is made towards other rare earth metals: Y, Dy, Er and Yb.

To examine the effect of substrate orientation on the Gd silicide phase growth and texture development, the phase formation sequence was monitored with *in situ* XRD measurements were performed on poly-crystalline Si, Si(100) and Si(111) oriented substrates. The XRD measurements are shown in Fig. 3, using a logarithmic gray scale, as a function of temperature. Since the detector only covers diffracted x-rays in a range of 14° in 2θ , two anneals were performed for each system to cover the range of $35 - 49^\circ$ and $48 - 62^\circ$ reducing ambiguity in phase identification.

We observe that the phase sequence due to the solid state reaction between Gd and Si is similar for all studied substrates. The as-deposited Gd,

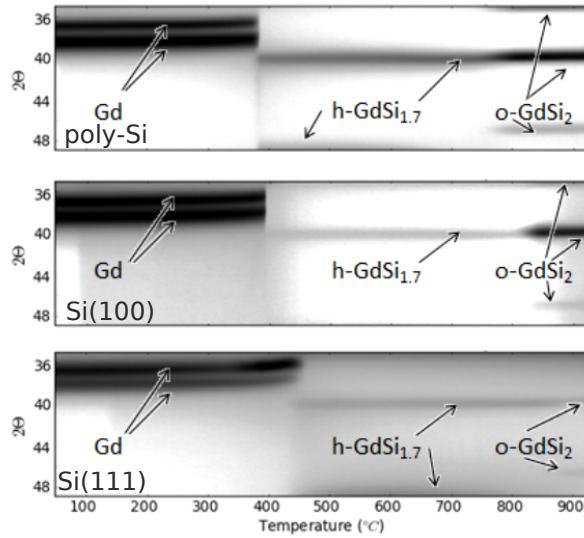


Figure 3: In situ XRD results of the solid state reaction between a 100 nm Gd film and poly-crystalline Si, Si(100) and Si(111) during a 3°C/s ramp anneal.

observed with peak positions consistent with the hexagonal lattice structure, transforms into the hexagonal $\text{GdSi}_{1.7}$ structure upon annealing. This hexagonal silicide subsequently transforms to orthorhombic GdSi_2 at higher temperature, which remains stable up to the highest temperature achieved, i.e. 950 °C. However, the differences between the substrates are clear when we focus on the temperature of silicide formation and on the relative intensities of the diffraction peaks. Both silicides, hexagonal and orthorhombic, are formed at lower temperatures on poly-Si, followed by Si(100) whereas Si(111) exhibits the highest formation temperatures. For comparison, we define the formation temperature T_{form} of a certain phase as follows: the temperature at which the total intensity of the phase's XRD-peaks increases maximal, e.g. the maximum of the first derivative of the total intensity of the relevant XRD peaks. The error of this temperature is taken as the full width at half maximum of this first derivative. In this consensus, the formation of $\text{h-GdSi}_{1.7}$ is observed at 380, 400 and 440 °C and the formation of o-GdSi_2 occurs at 795, 850 and 870 °C for poly-Si, Si(100) and Si(111), respectively. Thus, the lowest T_{form} for both hexagonal and orthorhombic are observed for poly-Si, whereas the highest T_{form} are found for growth on Si(111). Si(100) can be considered as an intermediate case.

The second dissimilarity between the solid state reaction on the different

substrates can be seen in the variation of peak intensities. This indicates that the formed silicides exhibit differences in texture with respect to the substrate orientation. To investigate this in more detail, *ex situ* pole figure measurements were performed on samples quenched at 750 °C (h-GdSi_{1.7}) and 950/1050 °C (o-GdSi₂) on Si(100) and Si(111) during an *in situ* XRD measurement. These pole figures are displayed in Figs. 4, 5 6 and 7 and the features on the pole figures can then be used to identify the various types of preferred orientation that are present in the film. In general, four primary types of texture components can be identified by pole figure measurements: random texture, fiber texture, axiotaxy and epitaxy [11]. The pole figures in this article contain only feature random and epitaxial oriented grains. Where random texture one shows itself in pole figures as a uniform background, an epitaxial structure has a clear recognisable structure in pole figures. An epitaxial texture means that all of the grains of the thin film are oriented in the same direction with respect with the substrate. Due to the fixed orientation of the grains, the Bragg diffraction condition is only satisfied for a discrete number of values for Φ and χ for each crystalline plane, resulting in high intense peaks in the pole figures.

Substrate	Out of plane orientation	In plane orientation	symbol color
Si(100)	h-GdSi _{1.7} (1100) // Si(001)	h-GdSi _{1.7} [0001] // Si[110]	yellow
	h-GdSi _{1.7} (1 $\bar{1}$ 00) // Si(001)	h-GdSi _{1.7} [11 $\bar{2}$ 0] // Si[$\bar{1}$ 10]	red
Si(111)	h-GdSi _{1.7} [0001] // Si[111]	h-GdSi _{1.7} (10 $\bar{1}$ 0) // Si($\bar{1}$ 12)	blue
Si(100)	o-GdSi ₂ (120) // Si(121)	o-GdSi ₂ (112) // Si(110)	green
Si(111)	Randomly oriented	Randomly oriented	-

Table 2: Overview of the preferential growth orientations for the hexagonal GdSi_{1.7} and orthorhombic GdSi₂ phase on respectively Si(100) and Si(111) together with the symbol color used in Figs. 4, 5 6 and 7.

For the thin films quenched at 750 °C (h-GdSi_{1.7}), one clearly observes these symmetrically distributed spots in the pole figures on Si(111) (Fig. 5), indicating an epitaxial growth of the hexagonal silicide phase on Si(111). The epitaxial alignment was identified and corresponds well with the alignment reported in literature [13] [14]. On the Si(100) substrate (Fig. 4), the observed features are two orders of magnitude smaller in diffraction intensity than those on Si(111), indicating a lower epitaxial quality or a higher amount of randomly oriented grains. For Si(100), the observed features can be linked to an epitaxial relationship suggested by Chen *et al.* [14] and Peto *et al.* [15]

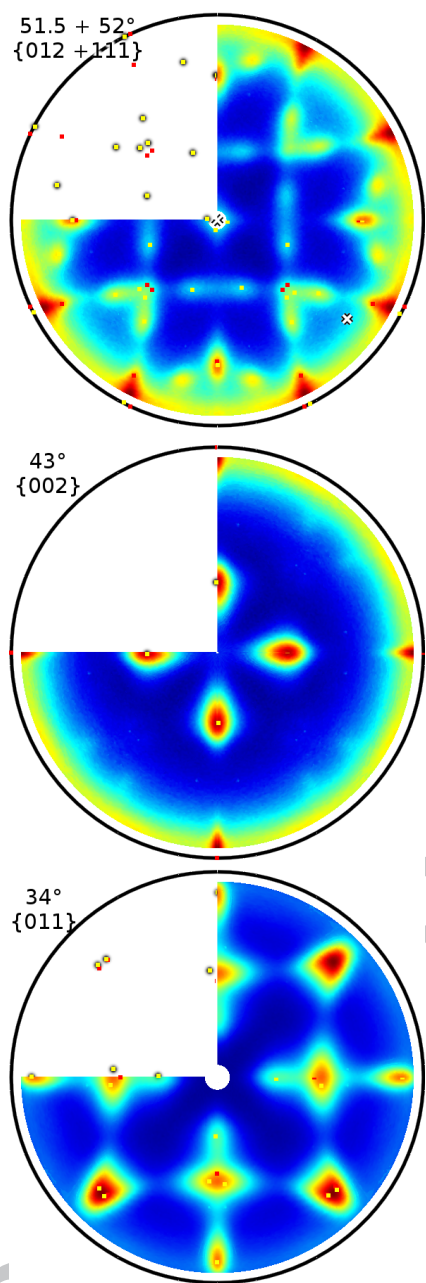


Figure 4: Overview of the XRD pole figures of an h-GdSi_{1.7} film on Si(100). The epitaxial relationships identified between the h-GdSi_{1.7} film and the Si substrate are indicated by coloured dots according to Table 2.

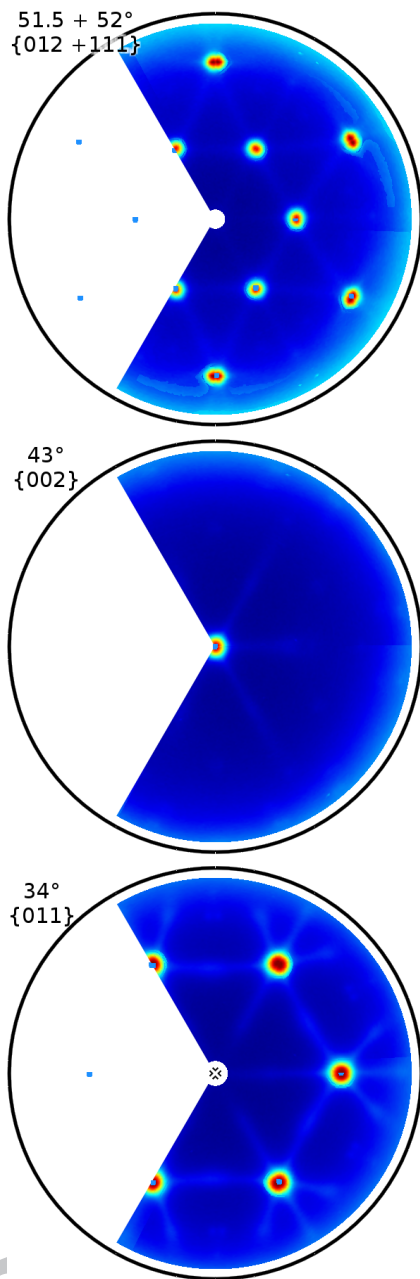


Figure 5: Overview of the XRD pole figures of an h-GdSi_{1.7} film on Si(111). The epitaxial relationships identified between the h-GdSi_{1.7} film and the Si substrate are indicated by coloured dots according to Table 2.

in which a side plane of the hexagonal unit cell lies parallel to the Si(100) substrate interface and the c-axis of this unit cell is oriented along one of two mutually perpendicular directions (i.e. h-GdSi_{1.7}(1 $\bar{1}$ 00) // Si(001) with h-GdSi_{1.7}[0001] // Si[1 $\bar{1}$ 0] (yellow dots) or h-GdSi_{1.7}[11 $\bar{2}$ 0] // Si[$\bar{1}$ $\bar{1}$ 0] (red dots)). The simultaneous appearance of these two epitaxial orientations in the silicide film is an additional indication of a lower uniformity in epitaxial growth.

Samples quenched in the o-GdSi₂ temperature region display no clear features for both substrates, indication that the o-GdSi₂ grains are randomly oriented. The random growth of o-GdSi₂ on Si(111) is evident (Fig. 7) as the faint epitaxial features present in the Si(111) pole figures can not be explained by preferential growth of o-GdSi₂. These features however are explained by including other crystalline phases. The most notable overlap occurs in its {112} pole figure as the {011} diffraction peaks of remaining epitaxial h-GdSi_{1.7} grains, both with very similar *d*-spacings of 0.1959 nm and 0.1994 nm respectively, are clearly visible (Fig. 7). On Si(100), faint features with a very low intensity are observed. These features can be linked to preferential growth of some o-GdSi₂ grains in the silicide film. However, the low intensity of these features together with the lower quality of the fit in Fig. 6 indicate that the quality of the epitaxial relationship between o-GdSi₂ and Si is much lower than between h-GdSi_{1.7} and Si. The epitaxial relationship as reported in Table 2 on Si(100) differs from the epitaxial relationship o-GdSi₂(001) // Si(001) with o-GdSi₂[100] // Si[110] reported by Gerocs *et al.* [16]. However, based on the findings of Molnar *et al.* [17] and Peto *et al.* [15], who suggested that the reported epitaxial relationship is only valid for metal films with a thickness below 30 nm, the difference in texture can be attributed to the metal film thickness which was selected for our experiments (i.e. 100 nm).

To conclude the results for the texture of Gd RES, we have found that there is preferred orientation of h-GdSi_{1.7} on both Si(111) and Si(100). The epitaxial quality is the highest on Si(111), which is also the substrate where h-GdSi_{1.7} is observed with the highest formation temperature. This is in agreement with the results of Jin *et al.* [18] who reported a correlation between vacancy ordering with increasing phase formation temperature.

3.2. Comparative study between different RE

Fig. 8 shows recorded XRD-measurements for each of the RE-elements on Si(111). We observe that almost all RE-metal films are detected with a hexagonal lattice after deposition (Bragg-peaks are outside the 2θ range of

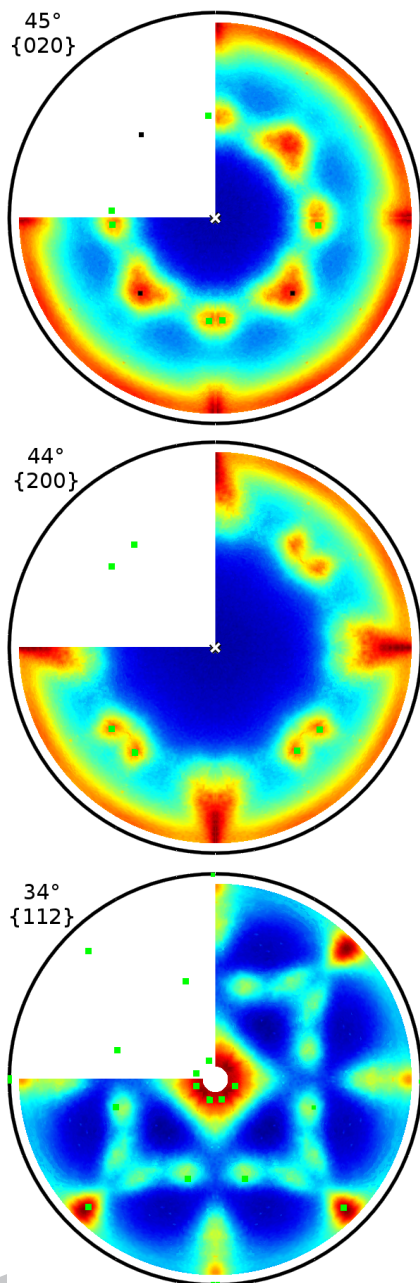


Figure 6: Overview of the XRD pole figures of an o-GdSi₂ film on Si(100). The epitaxial relationships identified between the o-GdSi₂ film and the Si substrate are indicated by coloured dots according to Table 2 whereas peaks originating from the Si substrate peaks are shown in black.

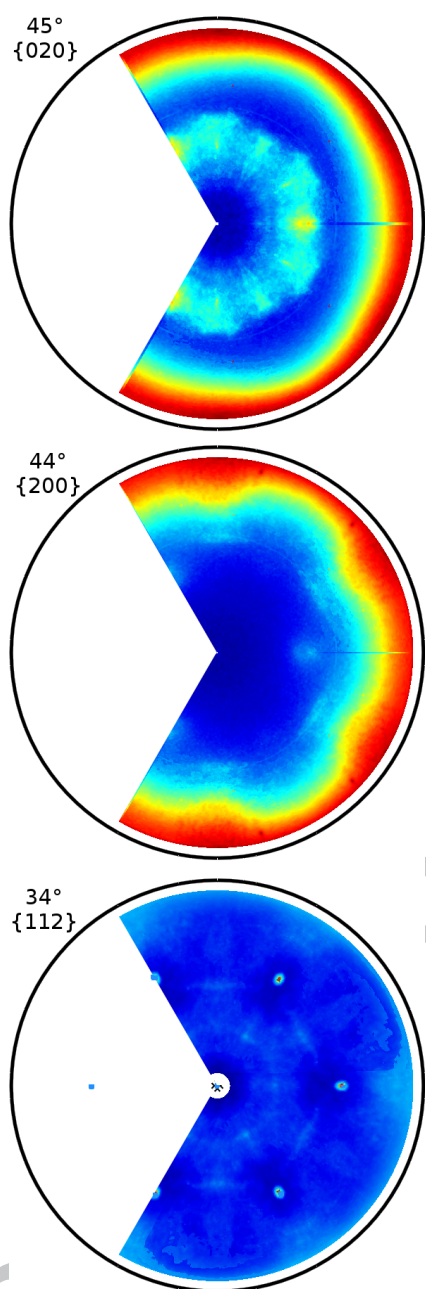


Figure 7: Overview of the XRD pole figures of an o-GdSi₂ film on Si(111). No preferential growth orientation could be identified. The epitaxial features indicated in blue are the result of the hexagonal GdSi_{1.7} phase.

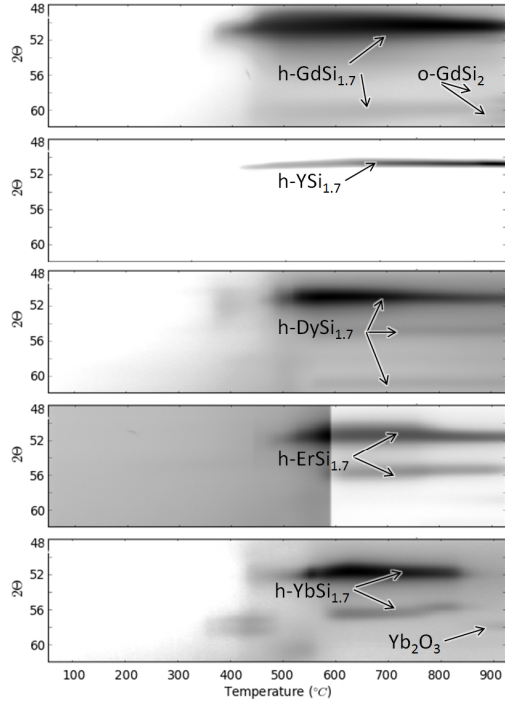


Figure 8: *In situ* XRD patterns for the 5 studied RE metals on Si(111). The different RE metals are ordered from top to bottom by decreasing lattice mismatch η (Table 1).

the measurements shown), except for Yb, for which a FCC crystal is identified as the low-temperature structure, in agreement with literature [19]. During the heating process, all RE-metals form the hexagonal $\text{RESi}_{1.7}$ structure from this as-deposited layer, as expected from the selection criteria of the different rare earth metals. In addition to this hexagonal $\text{RESi}_{1.7}$ phase, two other silicide phases are also observed during the anneal of Gd and Yb. The first one is the orthorhombic GdSi_2 phase, which we have discussed in the previous paragraphs. Based on the findings of Perri *et al.* [20], who reported that the formation temperatures for the orthorhombic silicide phase of Gd, Y and Dy is the lowest for Gd and the highest for Dy, it is possible that the transformation to the orthorhombic disilicide phase would occur for Y and Dy at temperatures higher than 950°C , the highest annealing temperature currently available in our set-up. Therefore it could be possible that orthorhombic Y and Dy silicide remains unnoticed during our *in situ* measurements.

An additional phase seems to form from the as-deposited Yb thin film at

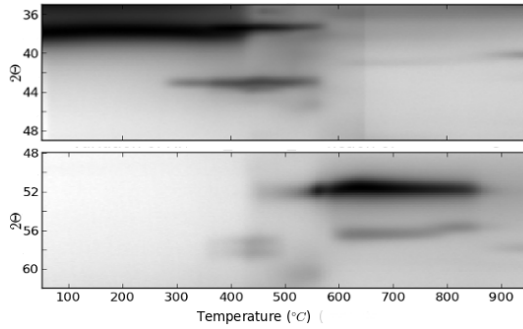


Figure 9: *In situ* XRD patterns for 100 nm Yb on Si(111).

a temperature of 300 °C on Si(111), which then transforms into hexagonal $\text{YbSi}_{1.7}$ at 580 °C. The phase has diffraction peaks at 2θ values of 27.5°, 35.6°, 38.0°, 44.0° and 58.7° (Fig. 9). However, our XRD-library could not provide a clear interpretation of these XRD-peaks was possible. One possibility is that the phase could correspond to a highly defective Yb_5Si_3 phase, although its XRD-peaks are reported for 2θ values of 29.7°, 36.5°, 38.9°, 44.4° and 57.4° for resp. the (200), (102), (210), (300) and (113) planes [21]. Another possibility that should be considered is that this intermediate phase is the result of some incorporation of impurities, like oxygen, due to non-ultra high vacuum conditions of the deposition process.

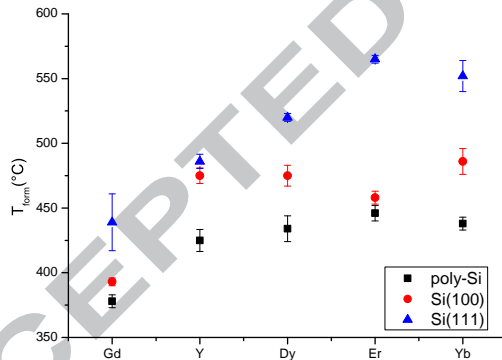


Figure 10: Measured formation temperatures of the hexagonal $\text{RESi}_{1.7}$ phase for Gd, Y, Dy, Er and Yb on poly-Si, Si(100) and Si(111).

Analogous measurements were performed on Si(100) and poly-Si. For

every sample, we observe the same phase sequence as observed on Si(111) but with other formation temperatures T_{form} . Since we are interested in the h-RESi_{1.7} phase, we summarise the results of these different XRD measurements in Fig. 10 by displaying the observed formation temperatures of the hexagonal RESi_{1.7} phase, with the formation temperatures calculated as explained in the experimental section. From these measurements, we can generalise the conclusion made at section 3.1 regarding the influence of the Si substrate on T_{form} : it is clear that the temperature at which RESi_{1.7} is formed is the lowest on poly-Si and the highest on Si(111) for all of the RE samples in this study.

Secondly, we observe a correlation between the formation temperature of h-RESi_{1.7} and the lattice parameters of the hexagonal plane, as described in Tab. 1, an observation which is the clearest on Si(111). The silicides with the smallest a lattice parameter (Gd, Y) form at lower temperatures than silicides with a larger lattice parameter (Er, Yb). However, the solid state reaction of Yb with Si differs from the other RE in several ways, with a different as-deposited crystal structure and an unknown phase preceding the formation of h-YbSi_{1.7} that is possibly related to the different deposition conditions of the Yb film.

4. Discussion

4.1. Influence of substrate orientation on formation of h-RESi_{1.7}

The formation of h-RESi_{1.7} is reported to be nucleation controlled for some RES systems[2], with Si as the dominant diffusing species. We shall now discuss the possible nucleation controlled silicide formation for our experimental results. According to the classical theory of nucleation, the formation is controlled by the nucleation barrier [10]:

$$\Delta G^{*} \sim \frac{\Delta\sigma^3}{\Delta G^2} \sim \frac{\Delta\sigma^3}{(\Delta H_{form} - T\Delta S)^2}$$

in which $\Delta\sigma$ corresponds to the difference in interface energy before and after nucleation, ΔH_{form} is the difference in formation enthalpy, T is the temperature and ΔS is the entropy change.

In our experiments, we have observed that h-RESi_{1.7} forms at higher temperature on Si(111) than on Si(100) or poly-Si. Pole figure measurements suggest that increasing epitaxial quality corresponds to an increasing formation temperature, thus confirming the work of Jin *et al* [18] and Molnar

[22] *et al.* This should indicate that the nucleation barrier is higher when h-RESi_{1.7} is grown epitaxially. However, we expect that the interface term, $\Delta\sigma = (\sigma_{M/MSi_{1.7}} + \sigma_{Si/MSi_{1.7}}) - \sigma_{M/Si}$, should give rise to a small value of $\sigma_{Si/MSi_{1.7}}$ for an epitaxial interface. It is clear that the higher nucleation barrier should be explained by another dominant effect, possibly a larger strain in h-RESi_{1.7} on Si(111), giving rise to a higher (i.e. less negative) formation enthalpy. Another explanation could be that the diffusion of Si becomes the controlling parameter due to lower availability of grain boundaries for epitaxial films. The latter could explain why Baglin *et al* reports nucleation mainly for the RES formed on Si(100) substrates [2].

4.2. Influence of substrate orientation on formation of o-RESi₂

The formation of orthorhombic GdSi₂ occurs at lower temperatures for poly-Si and Si(100) than for the Si(111) substrate. Due to the limited compositional change that is associated with the formation of orthorhombic GdSi₂ from h-GdSi_{1.7} [23], the driving force of this transformation is very small. As a result, the formation of o-GdSi₂ can be expected to be nucleation controlled and therefore governed by a nucleation energy barrier. Based on the pole figures of the o-GdSi₂ phase, a largely polycrystalline film is expected on all of the studied substrates with traces of an epitaxial relationship of a very low quality on Si(100). This implies that the magnitude of $\Delta\sigma$, the difference in surface energy before and after nucleation towards an orthorhombic phase, will increase with increasing epitaxial quality of the h-GdSi_{1.7} phase. This can explain the observed increase in o-GdSi₂ formation temperatures from poly-Si to Si(100) to Si(111) substrates (Fig. 3).

4.3. Formation of h-RESi_{1.7} for different RE

By comparing the formation temperatures of h-RESi_{1.7} for the different RES in this article, the *in situ* XRD measurements hints that there is a correlation between the lattice parameters of the hexagonal silicide phase from Table 1 and the formation temperatures of the h-RESi_{1.7} phase (Fig. 1). This can possibly be correlated with the the AlB₂ structure of h-RESi_{1.7}. Pearson [24] has reported that the stability of this crystallographic structure lies in the graphite-like net of Si-Si bonds. This was also reported by Vantomme *et al.* [9], who concluded from DFT-calculations that the RE-Si bonds are much weaker than the strong covalent Si-Si bonds. Since the Si-Si bond are weaker when the inter-atomic distance is larger, this stabilizing property scales with

the lattice parameter a (Table 1), thus giving a possible explanation for the observed trend.

5. Conclusion

The solid state reaction between 5 RE metals (Y, Gd, Dy, Er and Yb) and Si was studied using *in situ* XRD. The phases which form during the silicidation were identified during the reaction of a 100 nm RE metal film and a Si substrate.

For all metals studied, the formation of a hexagonal disilicide phase was observed on all substrates. The preferred grain orientation of this phase has been studied in detail for Gd on different crystalline Si substrates. The epitaxial quality is the highest on Si(111). Secondly, an orthorhombic Gd disilicide phase forms from the hexagonal phase and exhibits an epitaxial relationship on Si(100) but random growth is clearly more dominant and even is the only observable texture on Si(111).

The formation temperatures of h-RESi_{1.7} are the highest on Si(111) and the lowest on poly-Si for all examined RE metals. When comparing the different RE metals, an apparent correlation was found between the formation temperature of the h-RESi_{1.7} phase and the lattice parameter of this hexagonal phase.

6. Acknowledgments

The authors acknowledge the Fonds Wetenschappelijk Onderzoek Vlaanderen (FWO) for financial support. The KU Leuven contributed to this article in the context of the GOA/14/007 project. Use of the National Synchrotron Light Source, Brookhaven National Laboratory, was supported by the U.S. Department of Energy, Office of Science, Office of Basic Energy Sciences, under Contract No. *DE – AC02 – 76CH – 00016*.

References

- [1] F. Netzer, Rare earth overlayers on silicon, *Journal of Physics: Condensed Matter* 7 (6) (1995) 991.
- [2] J. Baglin, F. d'Heurle, C. Petersson, The formation of silicides from thin films of some rare-earth metals, *Applied Physics Letters* 36 (7) (1980) 594–596.

- [3] H. Norde, J. de Sousa Pires, F. d'Heurle, F. Pesavento, S. Petersson, P. Tove, The Schottky barrier height of the contacts between some rare-earth metals (and silicides) and p-type silicon, *Applied Physics Letters* 38 (11) (1981) 865–867.
- [4] J. Knapp, S. Picreux, C. Wu, S. Lau, Epitaxial growth of rare-earth silicides on (111)Si., *Applied Physics Letters* 48 (7) (1986) 466.
- [5] Y.-L. Jiang, Q. Xie, C. Detavernier, R. Van Meirhaeghe, G.-P. Ru, X.-P. Qu, B.-Z. Li, A. Huang, P. K. Chu, Oxidation suppression in Ytterbium silicidation by Ti / Ti N bicapping layer, *Journal of Vacuum Science & Technology A: Vacuum, Surfaces, and Films* 25 (2) (2007) 285–289.
- [6] A. Falepin, Phase transitions in epitaxially stabilized silicides on Si(111), Ph.D. thesis, K.U. Leuven (2003).
- [7] K. Maex, M. Van Rossum, Properties of metal silicides, INSPEC, the institution of Electrical Engineers, London, UK, 1995.
- [8] Handbook of Binary Alloy Phase Diagrams (CD Version 1.0), ASM International, ISBN PC - 0-87170-562-1, 1996.
- [9] A. Vantomme, M. Wu, S. Hogg, U. Wahl, W. Deweerdt, H. Pattyn, G. Langouche, S. Jin, H. Bender, Stabilisation and phase transformation of hexagonal rare-earth silicides on Si (111), *Nuclear Instruments and Methods in Physics Research Section B: Beam Interactions with Materials and Atoms* 147 (1) (1999) 261–266.
- [10] F. M. d'Heurle, Nucleation of a new phase from the interaction of two adjacent phases: Some silicides, *Journal of Materials Research* 3 (1988) 167–195.
- [11] S. Gaudet, K. De Keyser, S. Lambert-Milot, J. Jordan-Sweet, C. Detavernier, C. Lavoie, P. Desjardins, Three dimensional reciprocal space measurement by x-ray diffraction using linear and area detectors: Applications to texture and defects determination in oriented thin films and nanoprecipitates, *J. Vac. Sci. Technol., A* 31 (2) (2013) 021505–021505.
- [12] <http://www.cocoon.ugent.be/content/gustav>.

- [13] G. Molnar, I. Gerocs, G. Peto, E. Zsoldos, J. Gyulai, E. Bugiel, Epitaxy of $\text{GdSi}_{1.7}$ on (111)Si by solid phase reaction, Applied Physics Letters 58 (3) (1991) 249–250.
- [14] J. Chen, G. Shen, L. Chen, Interfacial reactions of Gd thin films on (111) and (001)Si., Apl. Surf. Sci. 142 (1999) 291–294.
- [15] G. Peto, G. Molnar, L. Dozsa, Z. Horvath, Z. Horvath, E. Zsoldos, C. Dimitriadis, L. Papadimitriou, Thickness dependent formation and properties of $\text{GdSi}_2/\text{Si}(100)$ interfaces, Appl. Phys. A 81 (2005) 975–980.
- [16] I. Gerocs, G. Molnar, E. Jaroli, E. Zsoldos, G. Peto, J. Gyulai, E. Bugiel, Epitaxy of orthorombic gadolinium disilicide on (100) silicon, Applied Physics Letters 51 (25) (1987) 2144–2145.
- [17] G. Molnar, G. Peto, E. Zsoldos, Z. Horvath, N. Khanh, The effect of silicon substrate orientation on the formation of Gd-silicide phases, Applied Physics Letters 102 (1996) 159–162.
- [18] S. Jin, H. Bender, M. Wu, A. Vantomme, H. Pattyn, G. Langouche, Epitaxial growth of Gd silicides prepared by channeled ion implantation, Journal of applied physics 81 (7) (1997) 3103–3107.
- [19] K. Gschneidner, L. Eyring, Handbook on the physics and chemistry of the rare earths, Vol. 1, Amsterdam, North-Holland, 1978.
- [20] J. Perri, I. Binder, B. Post, Rare earth metal disilicides., J. Phys. Chem. 63 (2006) 616–618.
- [21] Joint Committee on Powder Diffraction Standards (J.C.P.D.S.) 00-024-1025.
- [22] G. Molnar, I. Gerocs, G. Peto, E. Zsoldos, E. Jaroli, J. Gyulai, Thickness-dependent formation of Gd-silicide compounds, Journal of applied physics 64 (12) (1988) 6746–6749.
- [23] M. Wu, A. Vantomme, S. Hogg, H. Pattyn, G. Langouche, Channeled ion beam synthesis of heteroepitaxial $\text{Nd}_{0.32}\text{Y}_{0.68}\text{Si}_{1.7}$ layers, Applied physics letters 72 (19) (1998) 2412–2414.
- [24] W. B. Pearson, The crystal chemistry and physics of metals and alloys, Wiley-Interscience, 1972.

Solid-State reaction is studied of a several Rare Earth thin films with Si substrates.

h-GdSi_{1.7} grains have an epitaxial texture on both Si 100 and Si 111.

A correlation between formation temperature of h-RESi_{1.7} and lattice parameter of the hexagonal phase is suggested by the measurements

ACCEPTED MANUSCRIPT